JOURNAL OF AIRCRAFT
Vol. 48, No. 4, July–August 2011

Residual Stress Effects and Fatigue Behavior of Friction-Stir-Welded 2198-T8 Al-Li Alloy Joints

Yu E Ma*
Northwestern Polytechnical University, 710072 Xi'An, People's Republic of China
and
Phil Irving†
Cranfield University, Cranfield, England MK43 0AL, United Kingdom

DOI: 10.2514/1.C031242

Applications of friction stir welding in a fuselage structure were studied. Samples with two different friction-stir-weld orientations in the fuselage panel were tested: one is along the fuselage longitudinal direction and the other one is along the fuselage circumferential direction. Then fatigue cracks were investigated that were set in three different types: parallel and perpendicular to friction stir welds and between double welds. Sample geometries were machined from identical welds in order to remove the effect of the weld process on fatigue behavior. Tests were conducted on M (T) specimens with either longitudinal or transverse welds. Cracks growing into or growing away from the weld center, as well as in the nugget zone, were investigated. It is shown that fatigue crack growth for cracks growing away from the center seems similar to that of the parent material; for crack growing in the nugget, crack grows slower than in the parent material; and for cracks starting between double welds, the crack grows slower than in the other two types. The virtual crack-closure technique method was used to calculate stress intensity factor from residual stress (K_{res}) and effective R ratio in an attempt to explain the experimental findings.

Nomenclature

a	=	crack length
da/dN	=	crack growth rate
E	=	Young's modulus of elasticity
F_j	=	reaction force on the jth node
G	=	strain-energy release rate
K	=	stress intensity factor
K_{res}	=	stress intensity factor from residual stress
N	=	cycle (fatigue load)
R_{eff}	=	R ratio with the presence of residual stress
R_{nom}	=	applied load R ratio
t	=	thickness of samples
u_i	=	total displacement from the ith node
Δc	=	element size

I. Introduction

FRICTION stir welding (FSW) is an environmentally friendly manufacturing process with the potential for revolutionizing the aerospace industry. Friction stir welding is a solid-state joining process. The process can be described as a kind of local extrusion process. The parts to be joined are put in place and clamped firmly so that the welding tool can plunge into the material. Frictional heating and stirring of the pin and shoulder heats the material so that the material plasticizes just below the solidus temperature. As soon as the material is plasticized, the tool begins to move through the work pieces, stirring the metal and thereby achieving the weld. The process is autogenous, which means that no additional filler material is required, and it does not emit radiation, sparks, fumes, or chips. Friction stir welding can weld the unweldable and can be used to join the 2xxx and 7xxx series (mainly aircraft aluminum alloy). The process is simple, which makes it easy to use in aircraft manufacturing to replace the riveted joints, which can lead to weight and cost savings.

In the last decades, new design concepts for aircraft structures have been developed in order to reduce the weight and costs. The integral metallic structure with welding is one of the most promising. FSW is now considered mature for simple applications. It was shown that even for simple applications such as longitudinal fuselage joints, weight savings of up to 15% and cost savings of 20% can be achieved [1,2]. For example, in the case of the Eclipse 500, 263 welds replaced 7000 fasteners [3]. Therefore, a weld-integral structure will preclude initial cracks due to holes of the rivets; thus, the maintenance will benefit in terms of time and costs.

Burford et al. [4] described advances in friction stir welding for aerospace applications, summarized material and panel evaluations of friction-stir-welded 2xxx and 7xxx aluminum alloys and friction-stir-welding tool development, and pointed out that placing a continuous surface on a given scrolled shoulder improves surface roughness and in turn reduces the likelihood for fatigue to initiate in the central portion of the weld track. Kumar et al. [5] reviewed the applicability of FSW processing to aircraft applications and drew the conclusion that friction stir welding is gaining prominence as one of the principle joining techniques used in the aircraft industry. Kuwayama et al. [6] studied fatigue crack propagation properties of a friction-stir-welded 2024-T3 aluminum alloy. Donne et al. [7] and Cavaliere et al. [8] also studied residual stress due to friction stir welding and its effect on fatigue crack growth. Donne et al.'s [7] study included two different configurations: crack growth parallel with and perpendicular to the weld. The work included both friction-stir-welded alloy 2024 and alloy 6013, and an apparent improvement of the fatigue properties in the welded material was observed. As a new third-generation Al-Li alloy, the 2198-T8 alloy has a different chemical composition than those of 2xxx and 7xxx, and it has better properties, such as damage-tolerance properties that are 30% higher than the 2024 alloy and static mechanical properties that are about 20% higher than the 7075 alloy [9].

In the present work, traditional joints in fuselage structure were studied, and then possible applications of friction stir welding in a fuselage were developed and are shown in Fig. 1. FSW can be used

Received 19 September 2010; revision received 15 November 2010; accepted for publication 24 November 2010.

*Associate Professor, School of Aeronautics; ma.yu.e@nwpu.edu.cn.
†Professor, School of Applied Science. Member AIAA.

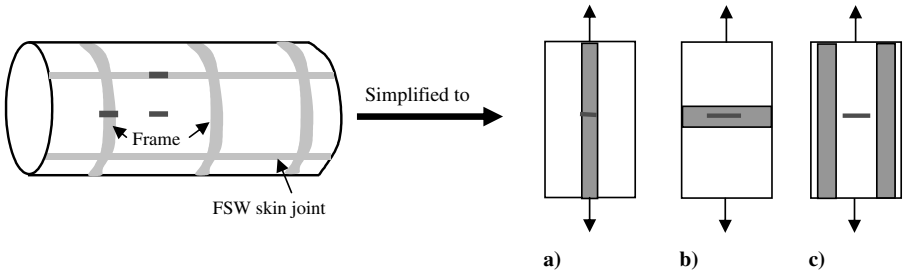

Fig. 1 Sample design for fuselage applications of FSW.

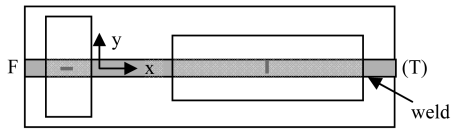

Fig. 2 Schematic showing types of M(T).

for window frame, longitudinal and circumferential fuselage joints, and so on. Alloy 2198-T8 was chosen in this work. Then test samples were designed, and fatigue behavior in FSW 2198-T8 Al-Li alloy joints were investigated for two different thicknesses and were compared with the parent material. To study the effect of different crack orientations on crack growth rate and fatigue life, three different types of specimens were tested and compared. Finite element models of all specimens were built, and subroutine programs were made to input residual stress profiles to finite element models. K_{res} was calculated by using the virtual crack-closure technique (VCCT) method [10], because the closure effect was taken into account in this method. K_{res} and R_{effctive} were compared.

II. Sample Preparation and Experimental Techniques

In Fig. 1, three different cracks were assumed in the FSW fuselage skin: one is a crack perpendicular to the weld, one is a crack parallel to the weld, and the last one is between double welds; the three different sample types were designed accordingly as designs a, b, and c.

Aluminium alloy 2198-T8 thicknesses of 1.6 and 3.2 mm sheets were chosen for all M(T) samples. Thickness effects on crack growth rate were neglected in this case. To remove the effect of the weld process on fatigue behavior, the same weld parameters were used to weld all sheets, so all samples had identical welds, and hence the hardness and microstructure were the same. Residual stress and weld are assumed to cause the difference of fatigue behavior in this work. Sample geometries were machined from the sheets welded in the same weld parameter, shown in Fig. 2. The sample size of M(T) is listed in Table 1.

Fatigue tests were performed on all samples according to procedures in ASTM E647 [11], in laboratory air at $R = 0.1$, with a load frequency of 10 Hz. Fatigue crack growth tests were also conducted on unwelded sheets at R ratios of 0.1 to be the baseline. Stress intensity factors for all specimens were calculated using the expressions recommended in ASTM E647 [11]. An automated optical video system was used to monitor crack growth for M(T) samples. Crack lengths could be monitored to an accuracy of 0.1 mm. LabVIEW 8.5 was used to monitor the optical system.

III. Experimental Results

A. Parent-Metal Fatigue Properties

To compare the welded results with unwelded results, fatigue crack growth tests were carried out in the parent material (without welds) at $R = 0.1$ and were compared with welded samples, shown in Fig. 3.

B. Fatigue Behavior of a Crack Perpendicular to the Weld

To keep the same applied stress level, all M(T) specimens were fatigue-tested at constant stress $\Delta\sigma = 44.6$ MPa and constant $R = 0.1$. For samples with a crack perpendicular to the weld and parent material, crack growth rates $\mathrm{d}a/\mathrm{d}N$ are shown versus $\Delta K_{\text{applied}}$ in Fig. 3. As shown in the graph, crack growth rates are very close to those of the base material, which means that residual stress has a small value in welded plates, even for two different thicknesses: 1.6 and 3.2 mm. There are two reasons for small residual stress: one is that the sample is very thin and the other is a 6-mm-long notch made across the middle of the weld that relaxed the residual stress significantly. There is small difference of residual stress distribution in different size samples, but the crack grows faster in the large sample than in the small sample when ΔK is smaller. For the thicker sample, 3.2 mm thick, the local maximum crack growth rate is 1.1×10^{-7} m/cycle at around $\Delta K_{\text{applied}} = 7.5$ MPa$\sqrt{\text{m}}$.

In Fig. 4, fatigue lives are compared for two thicknesses. The first thickness has a shorter life. For 550×200, fatigue life at 1.6 mm thickness is 1.5 times that at 3.2 mm thickness, and for 750×300, fatigue life at 1.6 mm thickness is 1.2 times that at 3.2 mm thickness. The difference of fatigue life mainly comes from thicker samples having a larger crack growth rate at the beginning, shown in Fig. 3. Residual stresses may lead to this.

C. Fatigue Behavior of a Crack Parallel to the Weld

For cracks parallel to the weld, the fatigue cracks grew along the weld centerline in the weld nugget. Figure 5 shows $\mathrm{d}a/\mathrm{d}N$ versus ΔK for 1.6 and 3.2 mm 2198 sheets. Crack growth rates of different sample sizes are similar, and are all slower than $\mathrm{d}a/\mathrm{d}N$ in the parent sheet. Pouget and Reynolds [12] also observed this effect. However, crack growth rate is similar to that of the parent material when $\Delta K_{\text{applied}}$ is smaller than 8.0 MPa$\sqrt{\text{m}}$.

Figure 6 shows 340,000 cycles of fatigue life for 550×200 and 620,000 cycles for 750×300.

D. Fatigue Behavior of a Crack Between Double Welds

For 3.2-mm-thick double welds at 550×200 and 750×300, two size specimens were studied, shown in Fig. 7. The locations of welds

Table 1 Sample size of M(T)

Type of sample	Sample size, mm: length by width by thickness	Sample amount
Crack perpendicular to weld	$550 \times 200 \times 1.6$; $750 \times 300 \times 1.6$ $550 \times 200 \times 3.2$; $750 \times 300 \times 3.2$	2 for each size
Crack parallel to weld	$550 \times 200 \times 3.2$; $750 \times 300 \times 3.2$	——
Crack between double perpendicular welds	$550 \times 200 \times 3.2$; $750 \times 300 \times 3.2$	——

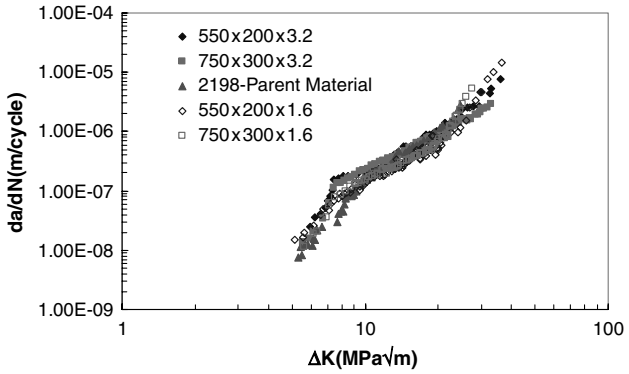

Fig. 3 Crack growth rates versus $\Delta K_{applied}$ for different sample sizes.

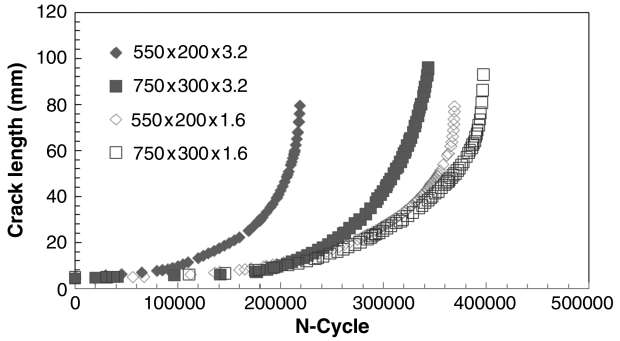

Fig. 4 Fatigue lives in samples with a single perpendicular weld.

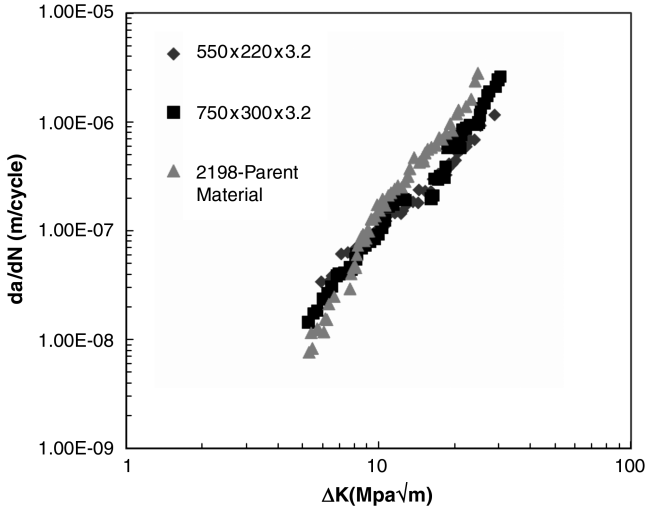

Fig. 5 Crack growth rates versus $\Delta K_{applied}$ for different sample sizes.

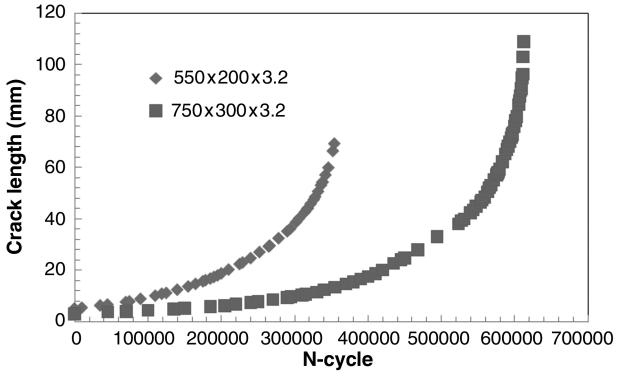

Fig. 6 Fatigue lives in 3.2 mm thickness with parallel welds.

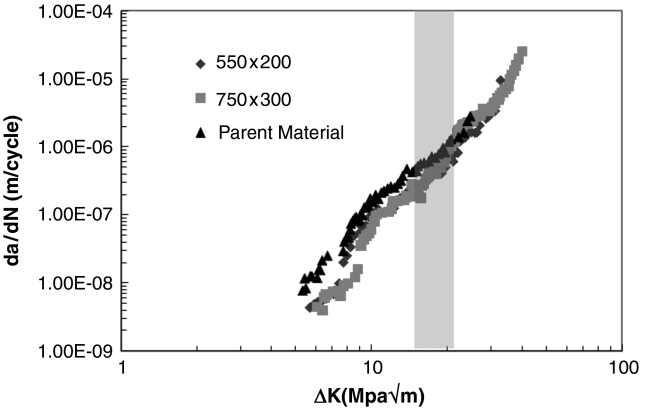

Fig. 7 Crack growth rate comparison.

in all specimens were the same: 50.0 mm away from the specimen centerline.

In Fig. 7, crack growth rates for both size samples are compared with the parent material. Both types of samples have similar growth rates and both are smaller than those of the parent material before the weld. After crossing the weld, growth rates increased a bit higher, close to those of the parent material, and the crack grew quickly until the specimen was broken.

At the shorter crack (e.g., shorter than 13.0 mm), crack growth rates are much smaller than those of the parent material. At a 10.0 mm crack length, the crack growth rate for 550×200 is two times smaller than that of the parent material, and at 750×300 it is six times smaller than that of the parent material.

E. Comparisons of Fatigue Behavior with Three Weld Types at 550 × 200

For the same thickness of 3.2 mm, specimens with three different types of welds (shown in Fig. 1) are all tested for sample size 550×200. All the tests were run at the same stress level and the same notch sizes. The comparisons are shown in Fig. 8.

Figure 8 shows crack growth rates for three weld types at 550×200. For a single perpendicular weld, crack growth rate is very close to that of the parent material after the crack grows across the weld zone. For a parallel weld, the crack grew in the weld centerline, the crack growth rate at the beginning is close to that of the parent material, and later is just half of that in the parent material. For a double weld, the crack growth rate is smaller than that of the parent material by about four times, but it will increase with a crack approaching the weld at around $\Delta K = 20$ MPa$\sqrt{\text{m}}$. After that, crack growth rate is close to that of the parent material, and crack growth rates always stayed smaller than that of the parent material for a parallel weld. This is because the crack grew in the nugget along the weld centerline. Here, the recrystallized process during welding caused finer grains. Normally, the finer grains increase crack growth rates, but a friction-stir-welded nugget is the reverse. Ma et al. [13]

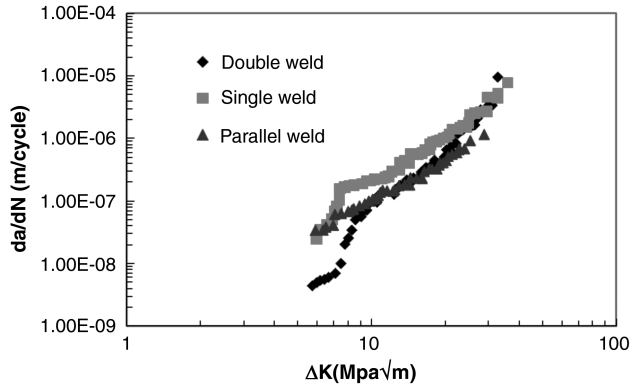

Fig. 8 Crack growth rates in three types of specimens.

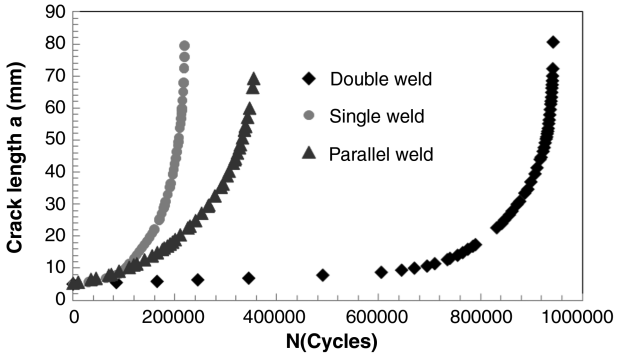

Fig. 9 Fatigue life in three types of specimens.

and Jata et al. [14] found the same phenomenon in another welded Al-Li alloy: the 2195-T8 nugget. During the weld, the nugget grain endures the coupling effects of three sides: material flow and thermal and mechanical aspects. The coupling effect causes grains in nuggets in different ways.

In Fig. 9, fatigue lives are compared in these three types of specimens. The double-weld specimen has the longest fatigue life, and the single perpendicular-weld specimen has the shortest one.

The fatigue lives of a double-weld specimen are three times and two times longer than the single perpendicular weld and parallel weld, respectively. The finite element analysis is used to explain the difference in the next section.

IV. Finite Element Analysis

For a friction-stir-welded structure, residual stress and microstructure both play an important role in crack growth rate [9,13,14]. It is well known that K_{res} is used to express the crack-tip stress intensity factor from residual stress. At present, there are two methods to attain K_{res}: one is determined by the cut compliance method [12,15–17] and the slitting method [18], and then residual stress distributions can be calculated by a discretization taking account of the weight function from K_{res}; another method is calculated by the weight function provided by Buechner [19], and many functions for different sample geometries produced by Glinka and Shen [20] or finite element method were used after the residual stress profiles were measured. For the weight function method, the main principle is

$$K_{res} = \int_{a_0}^{a} h(x,a) \cdot \sigma_{res}(x) \cdot \mathrm{d}x \tag{1}$$

where $h(x,a)$ is the weight function, which is available for several geometries and conditions, and $\sigma_{res}(x)$ is the residual stress distribution before crack propagation. However, redistributions of residual stress cannot be taken into account during the crack propagation if Eq. (1) is used to calculate K_{res}, which is mentioned in [21–24] as well.

To study the effect of residual stress on fatigue crack growth, two main methods are used: one is the superposition approach [7,8,12], and the other is the crack-closure model [21,24–28], originally proposed by Elber [29].

For the superposition approach, shown in Fig. 1, the total stress intensity factors $K_{max,tot}$ and $K_{min,tot}$ from both applied load and residual stress can be superposed together:

$$K_{max,tot} = K_{max,app} + K_{res} \qquad K_{min,tot} = K_{min,app} + K_{res} \tag{2}$$

The stress-intensity-factor range and effective stress ratio are calculated:

$$\begin{aligned}\Delta K &= K_{max,tot} - K_{min,tot} = (K_{max,app} + K_{res}) - (K_{min,app} + K_{res}) \\ &= K_{max,app} - K_{min,app} = \Delta K_{app}\end{aligned} \tag{3}$$

$$R_{eff} = \frac{K_{min} + K_{res}}{K_{max} + K_{res}} \tag{4}$$

The stress-intensity-factor range ΔK with the presence of residual stress is independent of the residual stress; however, the stress ratio R_{eff} is significantly affected.

Lam and Lian [21] show that there is about a four times difference for K_{res}, with and without considering the redistribution of residual stress. Lee et al. [23] and LaRue and Daniewicz [24] precisely predicted the fatigue life by crack-closure model after considering the redistribution of residual stress.

To study the redistribution of residual stress during crack propagations, finite element model was built for all M(T) samples in different sizes by using ABAQUS. A program was made to input the measured residual stress profiles to finite element models. K_{res} was calculated by the VCCT method [10] from the finite element model instead of the weight function method. The difference of K_{res} for different types of specimens comes from the difference of residual stresses.

A. Residual Stress Field

Residual stress profiles in 8.0-mm-thick samples measured by using the neutron diffractometer ARES-2 [17] at the Gesellschaft zur Förderung der Kernenergie in Schiffbau und Schiffstechnik were used in this analysis.

1. *Single Perpendicular Weld*

Figure 10 shows the residual stress profile in the sample with a single perpendicular weld. The residual stress presents a double-peaked shape, as in other researchers' work. The notch was made in the sample centerline, crossing through the weld. This means that the crack will initiate in the tensile residual stress zone. Tensile residual stress will increase the growth rate.

2. *Double Perpendicular Welds*

In Fig. 11, residual stress is assumed to be symmetric; the maximum residual stress is 120 MPa. The specimens are also

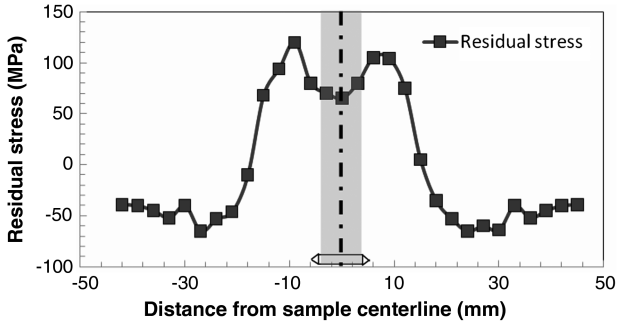

Fig. 10 Residual stress profile in a single-weld specimen.

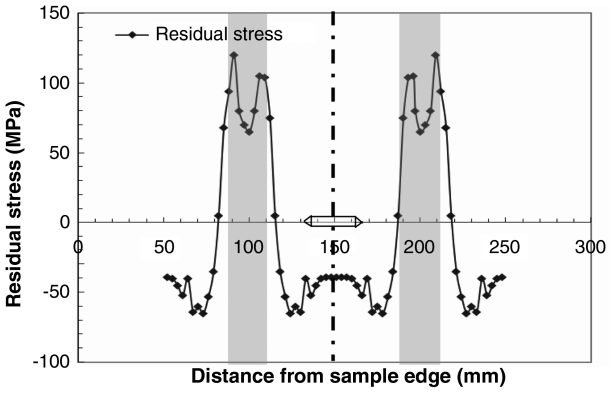

Fig. 11 Residual stress profile in a double-weld specimen.

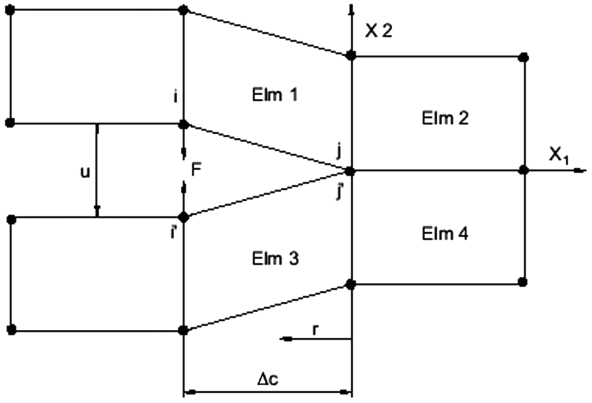

Fig. 12 Virtual crack-closure technique.

symmetric. The quarter finite element models were built to investigate the effect of residual stress. A 6.0-mm-long notch was made in the sample centerline as single perpendicular-weld samples; however, the notch is in the compressive residual stress zone for double-weld samples. Compressive residual stress will decrease crack growth rate, and it will be difficult to initiate a precrack in this zone. This explains why long fatigue cycles need to run for initiate a precrack when fatigue tests run on double-weld samples.

B. K_{res} Stress Intensity Factor from Residual Stress

To analyze the effect of residual stress on fatigue behavior, finite element analysis was used to calculate stress intensity factor K_{res} from residual stress by using ABAQUS. The VCCT method was used for calculating strain-energy release rate for unit thickness with the formulation:

$$G = \frac{F_j u_i}{2t\Delta c} \tag{5}$$

where F_j is the reaction force on $j$the node; u_i is the total displacement from $i$the node; t is thickness of samples and Δc is element size, see Fig. 12.

For plane stress, the relation between the strain-energy release rate and stress intensity factor is as follows:

$$G = \frac{K^2}{E} \tag{6}$$

If residual stress was input to the model, K_{res} can be attained from Eqs. (5) and (6).

Fatigue tests were run at a nominal R ratio, $R_{nom} = K_{min}/K_{max} = 0.1$, where K_{min} and K_{max} are the minimum and maximum stress intensity factor from applied stresses. However, residual stress exists in models, which changes the stress distribution in models. The superposition method introduced by Donne et al. [7,8] can be used to determine the effective R ratios by the Eq. (4).

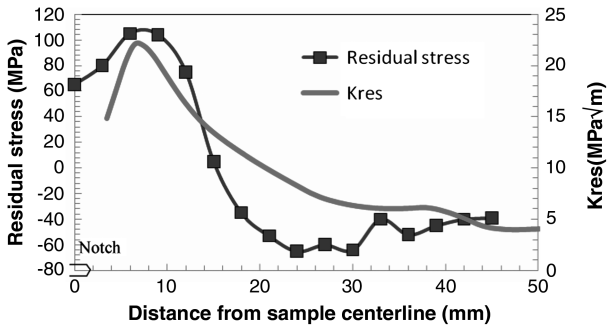

Fig. 13 Residual stress and K_{res} in single-weld specimens 750 × 300.

1. *Single Perpendicular Weld*

Because the specimen is symmetrical, the finite element model of a quarter-sample dimension was built to calculate K_{res}, shown in Fig. 13. K_{res} appears to follow the tendency of the residual stress distribution; it arrives at the maximum value of 22 MPa$\sqrt{m}$ at around the maximum residual stress of 110 MPa. Then K_{res} decreases with the residual stress.

In Fig. 14, $K_{max,app}$, $K_{min,app}$, K_{res}, ΔK_{app}, $K_{max,tot} = K_{max,app} + K_{res}$, and $K_{min,tot} = K_{min,app} + K_{res}$ are shown. K_{res} presents and changes the shape of $K_{max,tot}$ and $K_{min,tot}$ from $K_{max,app}$, $K_{min,app}$. $K_{max,tot}$ and $K_{min,tot}$ tend to be $K_{max,app}$ and $K_{min,app}$ with a decrease of residual stress.

R_{eff} was calculated by Eq. (4), shown in Fig. 15. The nominal applied R ratio is 0.1, but residual stress changes the nominal R ratio to even 0.7 at a 5.0-mm-long crack length. R_{eff} tends to be 0.1 with K_{res} decreasing.

2. *Double Perpendicular Welds*

K_{res} and residual stress for the 750 × 300 specimen are shown in Fig. 16. K_{res} is negative around the notch, then tends to be positive

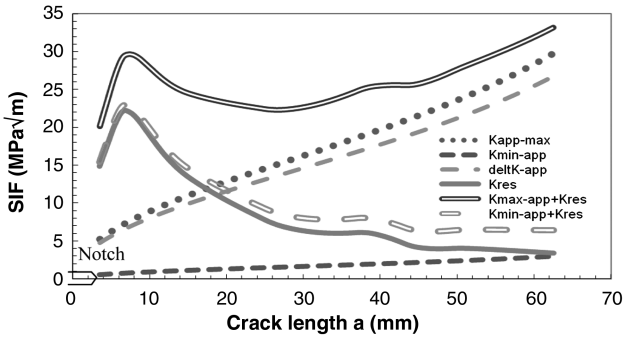

Fig. 14 Stress-intensity-factor (SIF) comparisons in single-weld specimens 750 × 300.

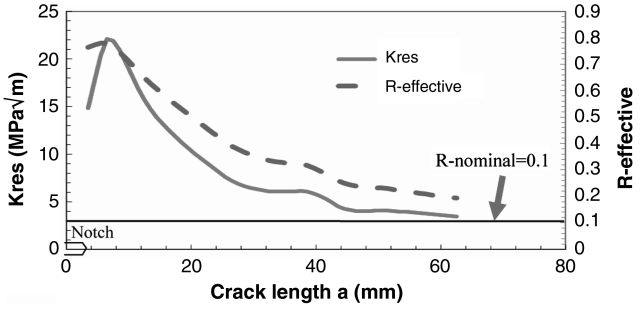

Fig. 15 Stress-intensity-factor comparisons in single-weld specimens 750 × 300.

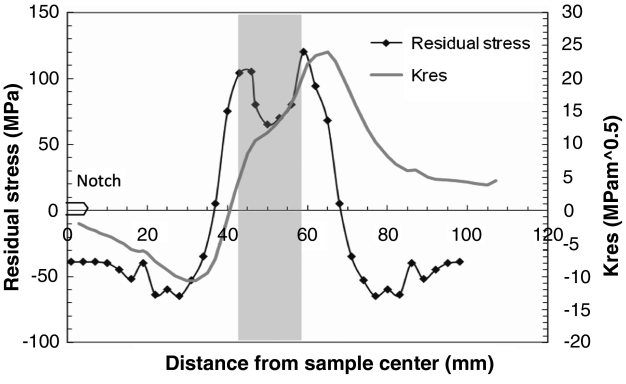

Fig. 16 Residual stress and K_{res}.

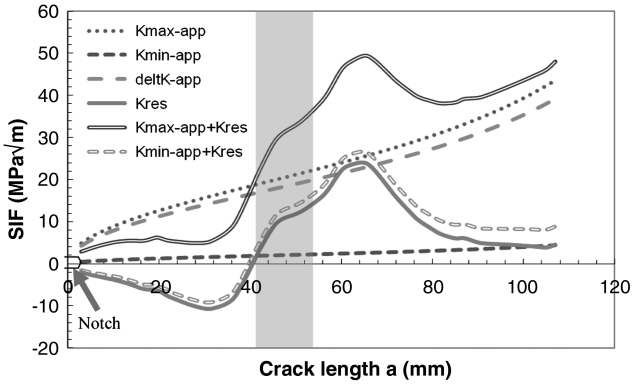

Fig. 17 Stress-intensity-factor comparisons 750 × 300.

with crack growing; the tendency of K_{res} is double-peaked as the residual stress distribution. K_{res} attains the two local maximums of 10 and 25 MPa$\sqrt{}$m at 45.0 and 62.0 mm, respectively.

In Fig. 17, $K_{max,app}$, $K_{min,app}$, K_{res}, ΔK_{app}, $K_{max,tot} = K_{max,app} + K_{res}$, and $K_{min,tot} = K_{min,app} + K_{res}$ are compared. K_{res} starts from a compressive value away from the notch tip. Changes in the shape of $K_{max,tot}$ and $K_{min,tot}$ from $K_{max,app}$, $K_{min,app} \cdot K_{max,tot}$ and $K_{min,tot}$ tend to be $K_{max,app}$ and $K_{min,app}$ with a decrease of residual stress effects. $K_{max,app}$, $K_{min,app}$, and ΔK_{app} linearly increase with an increase of crack length. However, the welded specimens present the residual stress. According to the superposition method, $K_{max,tot}$ and $K_{min,tot}$ totally changed the profiles of the stress intensity factor. At 62.0 mm, $K_{max,tot}$ reaches the maximum 50 MPa$\sqrt{}$m, much larger than $K_{max,app}$ at just 22 MPa$\sqrt{}$m.

R_{eff} versus crack length is shown in Fig. 18. The nominal applied R ratio is 0.1, but residual stress changes the nominal R ratio to even -1.7 at a 25.0-mm-long crack length. R_{eff} increases rapidly, because the crack grows close to the weld and tensile residual stresses that are present in the weld zone. After the crack grows through the weld, R_{eff} decreases into the nominal R ratio 0.1 with a decrease of K_{res}.

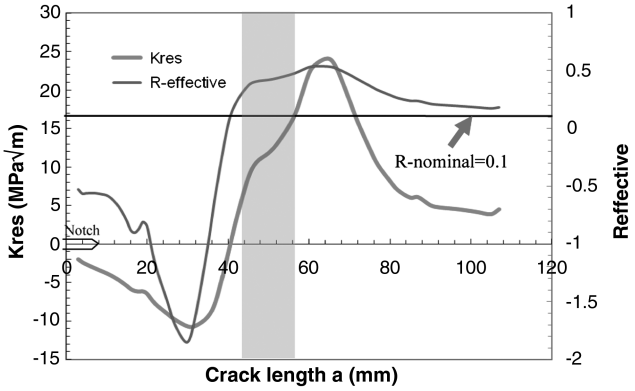

Fig. 18 R_{eff} in 750 × 300 double-weld sample.

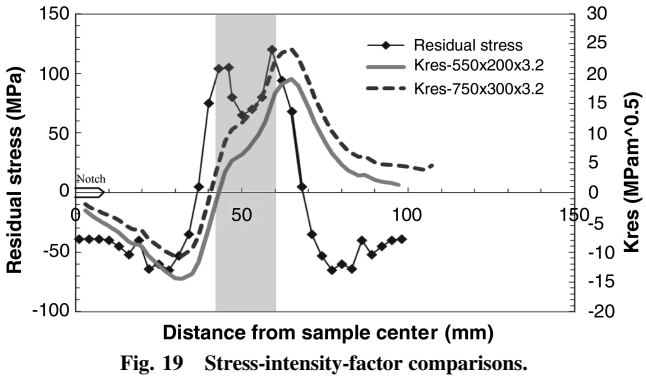

Fig. 19 Stress-intensity-factor comparisons.

3. Sample-Size Effects on K_{res}

In Fig. 19, K_{res} in both size specimens (750 × 300 and 550 × 200) are compared, and the profiles are similar to each other, but the larger sample has the larger value of K_{res}.

V. Conclusions

1) For 1.6-mm-thick samples with a single perpendicular weld, fatigue crack growth rate seems to be very similar to that of the parent material.

2) For 3.2 mm samples with a single perpendicular weld, fatigue crack growth rates for different sizes are very similar to each other and similar to that of the parent material. However, crack growth rate is larger than that of the parent material at small crack lengths. For samples with crack growth along the weld line, fatigue crack growth rates are slower than those of the parent material; sample size has little effect on crack growth rates. Samples with a double weld have crack growth rates that are much less than those of the parent material at the beginning of crack length and increase rapidly with a crack growing close to the weld, where residual stress is tensile stress. The fatigue lives of a double-weld sample and parallel-weld sample are 4.5 times and 2 times that of the single-weld sample.

3) A finite element model was used to calculate K_{res} and R_{eff}. K_{res} starts from a positive value for a single weld, and K_{res} starts from a negative value for a double weld. $K_{max,tot}$ and $K_{min,tot}$ change with K_{res}. All of these lead to less crack growth rate in the double-weld sample and the larger crack growth rate in the single-weld sample.

Acknowledgments

This paper is sponsored by the National Natural Science Foundation of China (11002111) and the Basic Research Project of Northwestern Polytechnical University (JC201021). Grateful thanks to the Cost-Effective Integral Structures project.

References

[1] Talwar, R., Bolser, D., Lederich, R., and Bauman, J., "Friction Stir Welding of Airframe Structures," *Proceedings of the Second International Symposium on Friction Stir Welding*, Gothenburg, Sweden, June 2000.

[2] Lohwasser, D., "Application of Friction Stir Welding for Aircraft Industry," *Proceedings of the Second International Symposium on Friction Stir Welding*, Gothenburg, Sweden, June 2000.

[3] Christner, B., "A Cooler Weld: An Emerging Joining Technology Lets Manufacturers Rethink How Products Fit Together," *Mechanical Engineering-CIME* [online journal], March 2003, http://www.allbusiness.com/professional-scientific/scientific-research-development/491898-1.html.

[4] Burford, D., Widener. C., and Tweedy, B., "Advances in Friction Stir Welding for Aerospace Applications," 6th AIAA Aviation Technology, Integration and Operations Conference (ATIO), Wichita, KS, AIAA Paper 2006-7730, 25–27 Sept. 2006.

[5] Kumar, B., Widener, C., Jahn, A., Tweedy, B., Cope, D., and Lee, R., "Review of the Applicability of FSW Processing to Aircraft Applications," 46th AIAA/ASME/ASCE/AHS/ASC Structures, Structural Dynamics, & Materials Conference, Austin, TX, AIAA Paper 2005-2000, 18–21 April 2005.

[6] Kuwayama, K., Asakawa, M., and Fujita, S., "Fatigue Crack Propagation Property of Friction Stir Welded 2024-T3 Aluminium Alloy," 50th AIAA/ASME/ASCE/AHS/ASC structures, Structural Dynamics, and Materials Conference, Palm Springs CA, AIAA Paper 2009-2619, May 2009.

[7] Donne, C. D., Biallas, G., Ghidini, T., and Raimbeaux, G., "Effect of Weld Imperfections and Residual Stresses on the Fatigue Crack Propagation in Friction Stir Welded Joints," *Proceedings of the Second International Symposium on Friction Stir Welding*, Gothenburg, Sweden, June 2000.

[8] Donne, C. D., and Raimbeaux, G., "Residual Stress Effects on Fatigue Crack Propagation in Friction Stir Welds," *Tenth International Conference on Fatigue ICF10*, 2001.

[9] Cavaliere, P., Cabibbo, M., Panella, F., and Squillace, A., "2198 Al-Li Plates Joined by Friction Stir Welding: Mechanical and Microstructure Behavior," *Materials and Design*, Vol. 30, 2009, pp. 3622–3631. doi:10.1016/j.matdes.2009.02.021

[10] Krueger, R., "The Virtual Crack Closure Technique: History, Approach and Applications," NASA CR-2002-211628, 2002.
[11] "Standard Test Method for Measurement of Fatigue Crack Growth Rates," ASTM International, ASTM E647, Washington, D.C., 2005.
[12] Pouget, G., and Reynolds, A. P., "Residual Stress and Microstructure Effects on Fatigue Crack Growth in AA2050 Friction Stir Welds," *International Journal of Fatigue*, Vol. 30, 2008, pp. 463–472. doi:10.1016/j.ijfatigue.2007.04.016
[13] MA, Y, E., Fisher, T., and Irving, P, E., "Size Effects on Residual Stress and Fatigue Crack Growth in Friction Stir Welded Al-Li Alloy 2195-T8 Joints," *International Journal of Fatigue* (to be published).
[14] Jata, K. V., Sankaran, K. K., and Ruschau, J. J., "Friction Stir Welding Effects on Microstructure and Fatigue of Aluminum Alloy 7050-T7451," *Metallurgical and Materials Transactions A: Physical Metallurgy and Materials Science*, Vol. 31, 2000, pp. 2181–2192. doi:10.1007/s11661-000-0136-9
[15] Fratini, L., Pasta, S., and Reynolds, A. P., "Fatigue Crack Growth in 2024-T351 Friction Stir Welded Joints: Longitudinal Residual Stress and Microstructural Effects," *International Journal of Fatigue*, Vol. 31, No. 3, 2009, pp. 495–500. doi:10.1016/j.ijfatigue.2008.05.004
[16] Lafly, A. L., Donne, C. D., Biallas G., Alléhaux D., and Marie F., "Role of Residual Stress on Fatigue Crack Propagation of FSW 6056-T78 Aluminium Joints Under Various Technologies," *Materials Science Forum*, Vols. 519–521, July 2006, pp. 1089–1094. doi:10.4028/www.scientific.net/MSF.519-521.1089
[17] Pasta, S., Reynolds, A. P., and Frantini, L., "Residual Stress Effects on Fatigue Crack Growth in Ti-6-4 Friction Stir Welds," *Journal of Materials Engineering and Performance*, Vol. 16, No. 1, 2007, pp. 86–92. doi:10.1007/s11665-006-9013-z
[18] Milan, M. T., Bose Filho, W. W., and Tarpani, J. R., Malafaia, A. M. S., Silva, C. P. O., Pellizer, B. C., and Pereira, L. E.. "Residual Stress Evaluation of AA2024-T3 Friction Stir Welded Joints," *Journal of Materials Engineering and Performance*, Vol. 16, No. 1, 2007, pp. 86–92. doi:10.1007/s11665-006-9013-z
[19] Buechner, H. F., "Weight Functions for the Notched Bar," *Zeitschrift für Angewandte Mathematik und Mechanik*, Vol. 51, 1971, pp. 97–109. doi:10.1002/zamm.19710510204
[20] Glinka, G., and Shen, G., "Universal Features of Weight Functions for Cracks in Mode I," *Engineering Fracture Mechanics*, Vol. 40, No. 6, 1991, pp. 1135–1146. doi:10.1016/0013-7944(91)90177-3
[21] Lam, Y. C., and Lian, K. S., "The Effect of Residual Stress and Its Redistribution on Fatigue Crack Growth," *Theoretical and Applied Fracture Mechanics*, Vol. 12, 1989, pp. 59–66. doi:10.1016/0167-8442(89)90015-3
[22] Daniewicz, S. R., Collins, J. A., and Houser, D. R., "An Elastic-Plastic Analytical Model for Predicting Fatigue Crack Growth in Arbitrary Edge-Cracked Two-Dimensional Geometries with Residual Stress," *International Journal of Fatigue*, Vol. 16, Feb. 1994, pp. 123–133. doi:10.1016/0142-1123(94)90102-3
[23] Lee, Y. B., Chung C. S., Park Y. K., and Kim H. K., "Effects of Redistributing of Residual Stress on the Fatigue Behavior of SS330 Weldment," *International Journal of Fatigue*, Vol. 20, No. 8, 1998, pp. 565–573. doi:10.1016/S0142-1123(98)00024-3
[24] LaRue, J. E., and Daniewicz, S. R., "Predicting the Effect of Residual Stress on Fatigue Crack Growth," *International Journal of Fatigue*, Vol. 29, 2007, pp. 508–515. doi:10.1016/j.ijfatigue.2006.05.008
[25] Nelson, D. V., "Effects of Residual Stress on Fatigue Crack Propagation. Residual Stress Effects in Fatigue," ASTM International, ASTM STP 776, Washington, D.C., 1982, pp. 172–194.
[26] Newman, J. C., "A Crack Opening Stress Equation for Fatigue Crack Growth," *International Journal of Fracture*, Vol. 24, 1984, pp. 131–135.
[27] Newman, J. C., "Fratran-II: A Fatigue Crack Growth Structural Analysis Program," NASA TM 104159, Feb. 1992.
[28] Solanki K., Daniewicz S. R., and Newman J. C., "Finite Element Analysis of Plasticity-Induced Fatigue Crack Closure: An Overview," *Engineering Fracture Mechanics*, Vol. 71, 2004, pp. 149–171. doi:10.1016/S0013-7944(03)00099-7
[29] Elber, W., "The Significance of Fatigue Crack Closure," *Damage Tolerance in Aircraft Structures*, ASTM STP 486, ASTM International, Washington, D.C., 1971, pp. 230–242.